

3-D MICROSTRUCTURE CREATION USING ELLIPTICAL VIBRATION-ASSISTED MACHINING¹

D. E. Brehl, T.A. Dow
Precision Engineering Center
North Carolina State University
Raleigh, North Carolina, USA

INTRODUCTION

“Elliptical vibration-assisted machining” (EVAM) is a diamond-tool machining process that can be used to create 3-dimensional micro-structures. In EVAM, the tool tip is driven very rapidly through a small (tens of micrometers) ellipse at multi-kHz frequencies. This elliptical motion is superimposed on the normal tool feed motion. EVAM shows potential for fabrication of micro-scale devices with true 3-D geometry, with greater material and shape flexibility than lithography methods derived from the semiconductor industry. When feature tolerances of ~200 nm suffice, it is more economical than methods such as micro-electro-discharge machining, focused ion beam, or laser ablation. EVAM also avoids problems of tool deflection, chatter, runout, and vibration associated with chip-making processes like micro-milling [1]. Because the tool is cutting in the workpiece for only part of each elliptical cycle, average cutting forces, and tool wear from mechanical and chemical effects, are reduced compared to conventional machining [2].

To date, EVAM has mostly been used in turning or facing operations to create precision macro-scale parts such as optical quality flats and molds with complex but low-aspect ratio geometries. For example, Negishi [3] made an annular flat in silicon carbide with a surface roughness of < 7 nm RMS. Shamoto *et al* have used an ultrasonic EVAM system to create steel micromolds for high-sag and Fresnel lenses [4], flat and hemispherical steel mirrors [5], and groove structures in several brittle materials [6].

The Precision Engineering Center’s EVAM tool, the Ultramill, has been used to machine binary microstructures. These have feature heights of 500 nm to 1 μm above the background. The Angstrom symbols in Figure 1 are machined in hard-plated copper. The large feature is 1 mm x 1 mm and was made with a 1 mm nose radius

tool. The small Angstrom symbol (inset in Figure 1) is shown to the same scale, and is 200 μm x 200 μm. It was made using a tool with a 50 μm nose radius. Its smallest feature (vertical bar on the topknot symbol) is only 15 μm across. The Angstrom symbols have RMS surface roughness of 15-25 nm and are seen to be burr-free when imaged by SEM. The thunderbird logo in Figure 2 was machined in 17-4 stainless steel using a 1 mm nose radius tool. It is approximately 1.08 mm x 1.08 mm, with surface roughness of 20 nm RMS with burr-free edges.

The goal of the current research is to use EVAM to create complex microstructures with features representative of micromolds and MEMS devices. Objectives to be achieved are a minimum feature resolution of 1 μm, 1:1 vertical aspect ratio, and an ability to create structures with both sculpted 3-D geometry and straight, steep sidewalls. If microstructures meeting these criteria can successfully be machined in previously intractable materials such as steel, glass, or brittle optical materials, then EVAM will provide an important addition to existing MEMS fabrication methods based on lithography, LIGA, or soft polymer molding techniques.

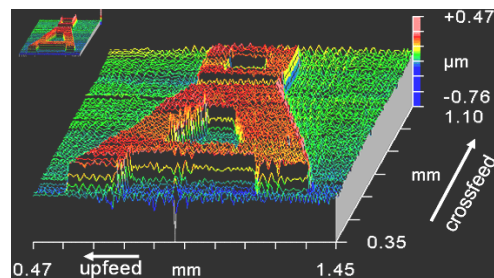


FIGURE 1. Interferograms of 1 mm x 1 mm (main image) and 200 μm x 200 μm (inset) Angstrom symbols machined by EVAM. Hard plated copper material [7].

¹ Research sponsored by NSF grant DMI-0423315, monitored by G. Hazelrigg.

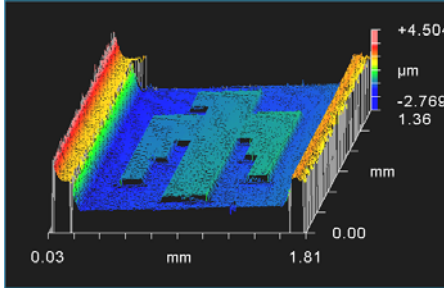


FIGURE 2. Interferogram of “thunderbird” machined in 17-4 stainless steel using EVAM.

PROCESS

Figure 3 shows how EVAM can be achieved using two parallel piezoelectric actuators to drive a diamond tool. Applying cyclic voltages to the stacks causes them to change length in a cyclical manner. The toolholder acts as a linkage to convert the linear stack motion into an elliptical path. By changing the voltage amplitude and/or phase difference between the stacks, the ellipse geometry (aspect ratio, tilt, and dimensions) can be varied through a wide range.

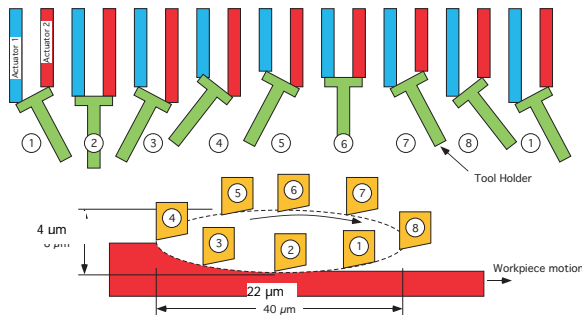


FIGURE 3. Ultramill EVAM concept

Figure 4 shows the tool motion in EVAM for two consecutive cutting cycles. During each cutting cycle, the work advances relative to the elliptical tool path. The overlapping toolpaths produce thin chips, resulting in greatly reduced tool forces compared to conventional cutting.

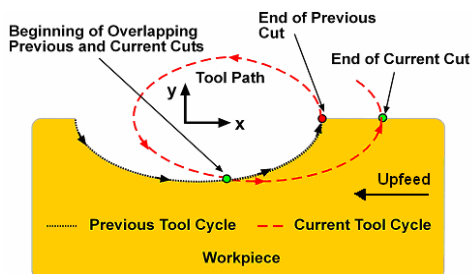


FIGURE 4. EVAM process cycle

Chip geometry is affected by the ratio between depth of cut and the ellipse vertical amplitude. When the depth of cut is equal to or smaller than the ellipse vertical amplitude, the tool exits the workpiece before completing its elliptical pass and small discontinuous chips are produced. When the depth of cut is greater than the ellipse vertical amplitude, the chip remains attached to the workpiece. A long discontinuous chip is produced with evenly spaced attached segments corresponding to the discontinuous chips in the preceding case. To create features that have a significant dimension in the depth direction, roughing passes can be made at a DOC larger than the semi-minor axis of the tool path ellipse. This economically achieves most of the required material removal. A finish pass is then made with DOC smaller than the ellipse semi-minor axis, to complete the part with excellent surface finish and sub-micrometer feature tolerance.

In EVAM the theoretical surface roughness in the upfeed direction is a function of the ellipse size and the upfeed increment, $F_{UP} = V/f$, where V is the workpiece velocity and f is the vibration frequency. The smaller the value of F_{UP} , the smaller is the theoretical feature height caused by the geometry of overlapping elliptical tool passes. When raster machining microstructures, axis moves are typically only a few tens to a few hundreds of micrometers in length. In this situation, the maximum upfeed velocity attained during a move is limited by the axis acceleration. Peak velocity is generally less than 1 mm / sec, which means that a theoretical upfeed surface roughness of 1 nm PV can be achieved with a vibration frequency in the KHz range. EVAM at such a relatively low frequency means that vibratory forces generated by the Ultramill are well below the natural frequency of the DTM's axes. The input power and cooling requirement for the piezoelectric actuators are also reduced.

EQUIPMENT

Figure 5 shows a cutaway view of the Ultramill. The two piezoelectric actuators are cooled by a dielectric fluid circulating continuously through the steel chamber. The hollow lightweight ceramic toolholder rests on alumina pins on the tops of the piezo stacks. A diamond tool is cemented to the toolholder. The titanium diaphragm exerts preload force on the piezo stacks and seals the coolant chamber. The Ultramill operates at frequencies up to 4 kHz.

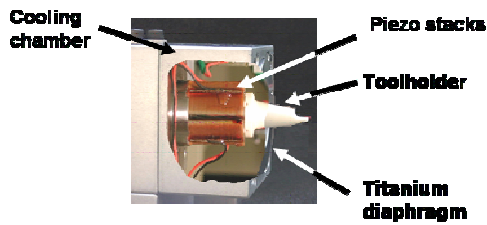


FIGURE 5. Ultramill EVAM tool

Figure 6 shows the Ultramill installed on a 3-axis diamond turning machine (DTM), which provides X-Y-Z motion for raster machining (the spindle is locked when using the Ultramill). The DTM's three axes are supported by hydrostatic oil bearings with nanometer-scale encoder resolution. The workpiece is held in place for machining by a vacuum chuck attached to the spindle. To facilitate touchoff, a video-microscope camera provides a view of the tool rake face and the work surface.

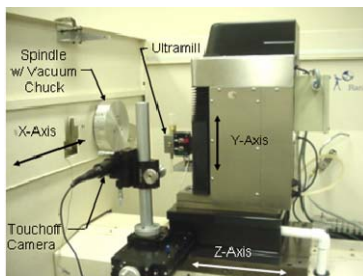


FIGURE 6. 3-axis diamond turning machine (DTM). Spindle is currently locked when using the Ultramill.

3-D MICROSTRUCTURES MADE USING ROUND-NOSED TOOLS

Several microstructures have been made with sculpted 3-D geometry, using round-nosed diamond tools.² Two representative parts are described here. In both cases the Ultramill was operated at a frequency of 1000 Hz with an elliptical toolpath of $22\ \mu\text{m} \times 4\ \mu\text{m}$ (long axis parallel to the work surface).

Convex Cylinder Section

Figure 7(a) shows an SEM image of a feature consisting of a convex cylindrical surface, oriented with its longitudinal axis parallel to the upfeed direction. The design cylinder radius is $1000\ \mu\text{m}$, with a chordal width of approximately $400\ \mu\text{m}$ and a length of $1\ \text{mm}$. From the flat background to the top of the cylindrical feature is

$20\ \mu\text{m}$. The part was machined with 3 sets of crossfeed passes at an increment of $5\ \mu\text{m}$. The first two sets of passes were for material removal with depth of cut $10\ \mu\text{m}$ and $9\ \mu\text{m}$ respectively, followed by a $1\ \mu\text{m}$ deep finishing pass. The part took 58 minutes to complete. Figure 7(b) is a white-light interferogram of the cylinder feature. A cross section was extracted from the interferometer data and a least-squares best-fit circle applied to estimate the radius of the convex portion of the machined feature. The residuals between the measured surface and the best fit radius approximately represent the outward normal surface profile of the part. These residuals give a crossfeed surface roughness of approximately $100\ \text{nm PV}$. This compares with a crossfeed surface roughness of $30\ \text{nm PV}$ in the flat portion of the part background. The theoretical crossfeed roughness derived from the tool radius and crossfeed increment is $3.1\ \text{nm}$. The surface roughness in the upfeed direction is $80\ \text{nm PV}$ along the crown of the convex segment and $42\ \text{nm PV}$ for the flat background. The theoretical upfeed surface roughness is $2.1\ \text{nm}$ based on the ellipse dimensions, upfeed velocity, and vibration frequency.

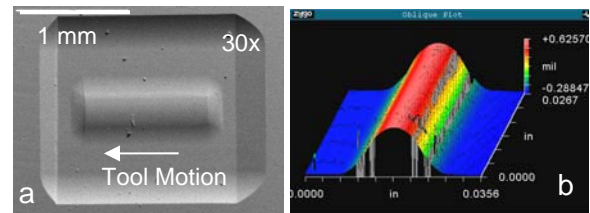


FIGURE 7. $1\ \text{mm}$ radius \times $20\ \mu\text{m}$ tall convex cylinder segment made with $1\ \text{mm}$ nose radius tool. (a) SEM image (b) Interferogram

Sculpted 3-D Groove Microstructure

Figure 8 shows the design of a microstructure consisting of parallel grooves with sculpted 3-D geometry. The grooves have a sinusoidal section in the crossfeed direction, which is superimposed on a cosine profile in the upfeed direction. The width (or wavelength) of each groove is $320\ \mu\text{m}$ and their maximum depth is $5\ \mu\text{m}$, giving an aspect ratio of 0.016. The length (or upfeed wavelength) of the part is $1.28\ \text{mm}$ while the amplitude of the sinusoidal section is $4.5\ \mu\text{m}$. The part was machined with a crossfeed spacing between raster passes of $5\ \mu\text{m}$. The part was made with a single set of crossfeed passes and took 51 minutes to cut.

² Diamond tools provided by Chardon Tool.

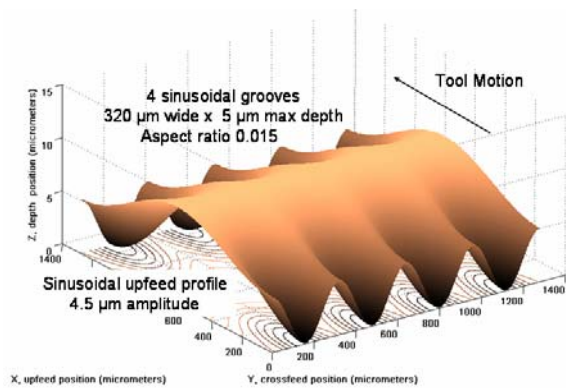


FIGURE 8. Design rendering of 3-D sculpted geometry microstructure made using 1 mm nose radius tool. Grooves have sinusoidal cross section and sinusoidal profile in upfeed direction.

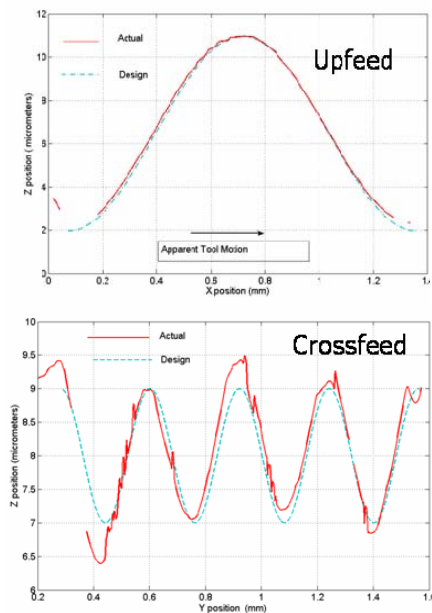


FIGURE 9. Profiles of part in Figure 11 from white-light interferometry data. (top) Upfeed profile (bottom) Crossfeed profile showing form error apparently caused by system thermal instability.

White-light interferometry was used to measure the sinusoidal groove part. The tilt of the surfaces was sufficiently shallow so that data could be obtained over almost the entire part. Figure 9 shows upfeed and crossfeed profiles made from the interferometry data. The upfeed profile was taken along the bottom of one of the grooves. In the upfeed direction the machined profile closely matched the intended profile. In the crossfeed direction, there is form error with one groove bottom and one ridge top being

displaced vertically by 500 nm. This form error resulted from slow thermal expansion and contraction of the Ultramill during the machining run, in the depth of cut direction. Corrective measures have been identified and the part will be recut.

SHARP-NOSE TOOLS

Round nose tools are limited to making low-aspect ratio features with shallow curved sidewalls. The minimum possible groove width for a round tool grows significantly with increasing depth of cut due to the rapid increase in chord width of the tool cross section. For example, a tool of 50 μm nose radius will cut a groove 20 μm wide at a 1 μm depth of cut, but for a 5 μm deep cut the groove width increases to 44 μm . The groove width defines the minimum crossfeed spacing of positive features.

Figure 10 shows an SEM image of a sharp nose tool with a 40° included nose angle. The cutting edges are on the sides of the tool. With such a tool, straight side walls can be made which are within 20° of vertical. For a 5 μm depth of cut, such a tool will produce a groove only 3.6 μm wide at its top. The tool in Figure 10 is “dead-sharp” with a nose radius less than 100 nm. For a crossfeed increment of 1 μm such a tool will produce a theoretical crossfeed surface roughness of 1373 nm PV. Most applications require much smoother finishes on horizontal or sculpted surfaces. Therefore a “hybrid” sharp-nose tool with a 1-2 μm nose radius may be more suitable. For example, a sharp-nose tool with 2 μm nose radius produces a theoretical crossfeed surface roughness of 62 nm at a crossfeed increment of 1 μm .

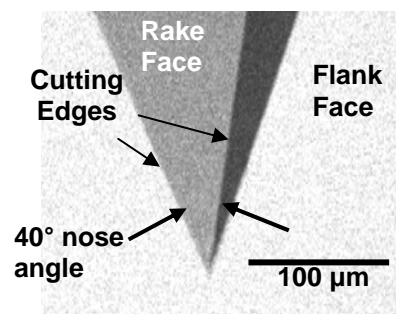


FIGURE 10. SEM image of a “dead sharp” diamond tool with 40° nose angle.

An important difference between round-nose and sharp-nose tools is the relative velocity between the cutting edge and the work material. For a round-nose tool, the angle between the

engaged portion of the cutting edge and the tool vertical centerline is almost perpendicular, for typical machining conditions where the depth of cut is small compared to the nose radius. The vertical portion of the elliptical tool motion has a component projected along the tool cutting edge that is essentially zero. This means that cutting is orthogonal, with the instantaneous rake angle determined by the instantaneous velocity vector (ie direction of the tangent to the elliptical tool path).

For a sharp-nose tool the angle between the cutting edge and vertical centerline is acute and equals half the tool nose angle. The projection of the vertical tool motion along the cutting edge is non-zero except at the instants when the tool reverses direction. This means there is a relative motion along the cutting edge between the tool and workpiece. The relative motion normal to the cutting edge is also non-zero and is at an angle to the tool's vertical centerline. From the perspective of the cutting edge, the tool-workpiece motion is 3-dimensional and cutting is non-orthogonal. Furthermore the direction and magnitude of these cutting edge relative velocity components change continuously as the tool moves through the machining ellipse. We are beginning to explore the ramifications of this 3-dimensional cutting edge motion. Cutting dynamics, chip formation and flow direction, kinematics, theoretical surface features, and tool wear could all be affected.

PARTS MADE USING SHARP-NOSE TOOLS

Trihedrons³

Figure 11 shows SEM images of trihedrons machined in hard-plated copper. This part was a master used for molding polymer corner cubes. The large trihedrons are 80 μm tall on a 112 μm side pitch. The small interstitial trihedrons are approximately 10 μm wide and show no burr at 4000x. These parts were created using a dead sharp diamond tool with an included angle of 70.6°, 0° rake angle, and 10° clearance angle. To make these parts, one set of parallel grooves was cut. The spindle was then rotated 60°, which also translated the part in X and Y since it was located away from the spindle center. The tool was moved to compensate for this translation and a second set of parallel grooves

machined. Another 60° rotation was made and the process repeated for the last set of grooves. The interstitial features were obtained by offsetting the center of the machining coordinate system from the spindle center of rotation by 5 μm . Each groove was made with a series of roughing cuts 10 μm deep, followed by a set of shallow finishing cuts to eliminate burrs.

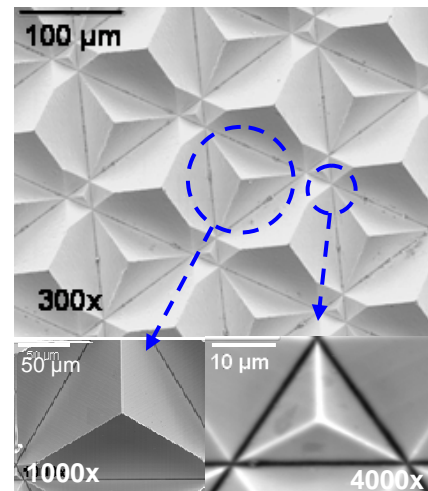


FIGURE 11. (Top) 80 μm tall trihedrons in plated copper. (Lower left) Detail of 80 μm trihedron (Lower right) Interstitial trihedron ~10 μm wide.

Microcontactor Pin⁴

Figure 12 shows the contactor element of a micro-relay. A sculpted 3-D groove pattern will be machined onto each of the contactor's three pins. The groove pattern is similar to that shown in Figure 8, except it is only 1/8 as large in the horizontal plane. These grooves have a sinusoidal cross-section with a spacing of 8 μm and a maximum depth of 5 μm , for an aspect ratio of 0.6. The grooves have a cosine profile in the upfeed direction with a length of 160 μm and an amplitude of 4.5 μm . The pin material is a composite of gold conductor material in a glass matrix.

This activity will demonstrate the ability of EVAM to modify an existing MEMS part or raw material blank. Besides the machining of such a small microstructure, challenges to address include part fixturing, positioning of the tool tip at precise locations on the part, and compensating for tilt between the part surface and DTM axes.

³ Trihedron project funded by Oak Ridge National Laboratory.

⁴ Microcontactor project funded by Sandia National Laboratories.

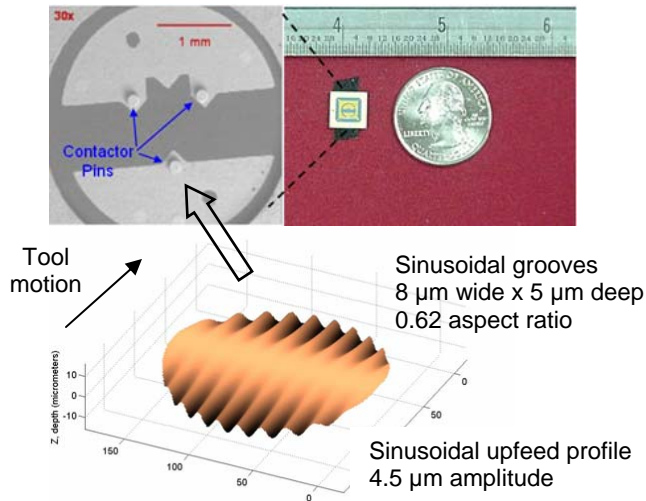


FIGURE 12. (Top) Microcontactor element (Bottom) Groove pattern with sculpted 3-D geometry, to be machined onto each pin.

Microgripper

To demonstrate an ability to fabricate functional microdevices with integrated mechanical and optical elements, the Ultramill will make the microgripper shown in Figure 13. The transparent polycarbonate gripping elements act as light pipes. As the gap between the gripper tines changes, the amount of light coupled through the gap changes proportional to displacement and confirmation of object capture. This provides feedback of gripper separation. When the gripper encounters an object, the light between the tines will be blocked. Successful operation of the gripper requires light pipe surfaces to be machined to an optical quality finish, to achieve total internal reflection. To facilitate fabricating the gripper's complex geometry, a rotational (C) axis will be added to the diamond turning machine, for precision angular positioning of the work relative to the tool tip.

To make the microgripper, the aluminum substrate flexure and polycarbonate gripper flexure will be rough cut by traditional process. EVAM will be used to machine an optical quality surface on the bottom face of the polycarbonate part which will then be cemented to the aluminum flexure. The assembly will be held on the DTM using a porous carbon vacuum chuck. The top polycarbonate surface will be faced using EVAM giving an optical quality surface. Next, EVAM with a sharp-nose tool will be used to machine the polycarbonate gripper flexure to the final geometry, with optical quality finishes

on the side surfaces. Finally the thermal actuator will be glued to the aluminum flexure to complete an integrated micro-optomechanical-electrical device.

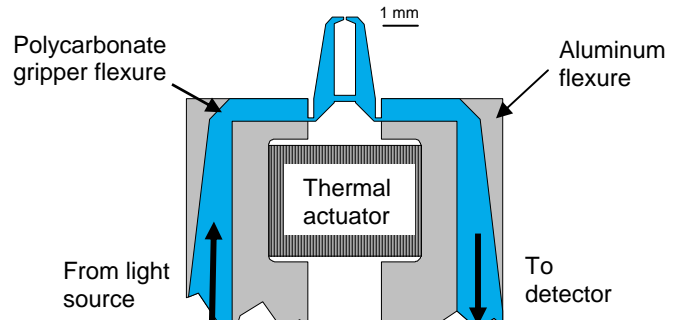


FIGURE 13. Microgripper assembly

CONCLUSIONS

The Ultramill EVAM tool has been used to create binary, sculpted 3-D, and trihedron microstructures up to 80 μm tall. Diamond tools with round and sharp nose geometry have been used successfully. Roughing and finishing passes can be used to achieve large depth dimension features while avoiding burr formation. Fabrication is planned of functional devices with complex geometry and requiring optical quality finishes.

REFERENCES

- [1] Benvides, G., "Meso-Machining Capabilities", M⁴: Workshop on Micro / Meso-Mechanical Manufacturing, Evanston, IL, May 2000.
- [2] Cerniway, M., "Elliptical Diamond Milling: Kinematics, Force, and Tool Wear", MS thesis, North Carolina State University, 2001
- [3] Negishi, N., "Elliptical Vibration-Assisted Machining with Single-Crystal Diamond Tools", MS thesis, North Carolina State University, 2003
- [4] Shamoto, E., "Ultraprecision Micromachining of Hardened Die Steel by Applying Elliptical Vibration Cutting", *JSME News*, v1:4, 2005
- [5] Shamoto, E., Suzuki, N., Tsuchiya, E., Hori, Y., Inagaki H., Yoshino, K., "Development of 3-DOF Ultrasonic Vibration Tool for Elliptical Vibration Cutting of Sculptured Surfaces", *Annals of CIRP*, v54:1, pp 321-324, 2005
- [6] Suzuki, N., Shinsuke, M., Makoto, H., Shamoto, E., "Ultraprecision Micromachining of Brittle Materials by Applying Ultrasonic Elliptical Vibration Cutting", *Proceedings 2004 Int. Symposium on Micro-NanoMechatronics and Human Science*, Nagoya University, pp 133-138
- [7] Brocato, B., "Micromachining Using Elliptical Vibration-Assisted Machining", MS thesis, North Carolina State University, 2005